Doping dependence of the thermopower of high-T_c cuprates: Tight-binding band model

Yoshimi Kubo
Fundamental Research Laboratories, NEC Corporation, 34 Miyukigaoka, Tsukuba 305, Japan
(Received 26 July 1993; revised manuscript received 21 December 1993)

Tight-binding calculatoins are performed which include both Cu-O and O-O interactions in the CuO_2 plane. These calculations reconcile inconsistencies in observed behaviors of the thermopower S and the Hall coefficient R_H: the sign of S of high-T_c cuprates at room temperature becomes negative in the overdoped regime, while R_H remains positive. A striking feature of the CuO_2 antibonding band is that a holelike Fermi surface is formed even when the band is less than half-filled. This brings about an unusual electron state in which the Hall (cyclotron) mass parallel to the Fermi surface is holelike (<0) but the transport mass perpendicular to it is *electronlike* (>0). This electronlike transport mass contributes to negative S, while the holelike Hall mass results in positive R_H. In such a state, the electron on the Fermi surface has complete duality: it is holelike in one direction, but electronlike in another. In the overdoped regime, where $R_H>0$ and $S<0$, the hole doping increases the carrier concentration defined as $\propto R_H^{-1}$, but it decreases the carrier concentration defined as $(n/m^*)_D$ in Drude's formula. This qualitatively explains the recent muon-spin-rotation (μSR) results that the superconducting carrier concentration $n_s/m^* \sim (n/m^*)_D$ decreases with hole doping in the overdoped regime.

INTRODUCTION

Transport properties of high-T_c cuprates in the normal state have been considered very puzzling.[1] In optimally doped high-T_c cuprates with maximum T_c's, the resistivity ρ and inverse Hall coefficient R_H^{-1} have linear relationships to temperature T, but the T dependence of the thermopower S is very weak. These results are different from those expected for a simple Fermi liquid, namely, T^2 dependence of ρ, T-independent R_H, and T-linear S.

However, recent studies on the *doping* dependence of these transport properties revealed two features which might offer a key to the solution of the puzzle. One is a T^2 law of the inverse Hall mobility $\mu_H^{-1} \sim T^2$ (or $\cot\theta_H \equiv \mu_H^{-1}/B$, where θ_H is the Hall angle and B is the applied field) observed in a wide doping range from the underdoped to the overdoped regime.[2-11] This is very surprising because the T dependence of ρ shows large variation from sublinear to superlinear with increasing doping level. Outside of the optimal doping range, ρ is no longer T linear. However, R_H^{-1} shows complicated nonlinear T dependence so as to hold the relation $\mu_H^{-1} \sim T^2$. This universal relation, observed in a wide doping range from the underdoped to the overdoped regime, clearly demonstrates the close correlation between ρ and R_H. The most straightforward interpretation of the relation $\mu_H^{-1} \sim T^2$ is that μ_H^{-1} represents the isotropic scattering rate τ^{-1} as in the usual expression $\mu_H^{-1} = m^*/e\tau$ for a parabolic band.[3] This is consistent with the band calculation which predicts a nearly parabolic hole band arising from the CuO_2 plane.[12] In this case, the scattering rate of the high-T_c cuprates is always $\sim T^2$, which is consistent with the Fermi-liquid picture.

Another remarkable feature is a general trend observed in the doping dependence of the thermopower S.[13-16] Plots of S at room temperature versus doping level for various high-T_c cuprates fall on a universal curve which decreases with doping and crosses $S=0$ at around optimal doping with maximum T_c. Thus the sign of S changes from positive to *negative* on going from the underdoped to the overdoped regime. However, this behavior appears to be inconsistent with that of the Hall coefficient R_H, which maintains positive values even in the overdoped regime.[3] If we use a parabolic hole-band model to explain the T^2 law of μ_H^{-1}, the sign of S must be positive over the entire range of doping. Thus it is difficult within a simple Fermi-liquid picture to explain both the facts of positive R_H and negative S observed in the overdoped regime.

On the other hand, the existence of the large Fermi surface predicted from the band calculation has been confirmed by photoemission experiments for both hole-doped[17] and electron-doped[18] systems. This strongly suggests that the Mott-Hubbard picture at half-filling is destroyed by a small doping and that the band picture with near half-filling is appropriate for the doped metallic phases. However, it is noted that the observed bandwidth is only about half of that calculated, which is probably due to the strong correlation effects. Therefore the band calculation correctly predicts the Fermi-surface morphology, while it fails in predicting the details of the band dispersion.

The purpose of this paper is to give a consistent explanation of the doping dependences of both R_H and S in terms of a tight-binding band model of the CuO_2 plane. The observed universalities in the transport properties strongly imply that the transport properties of high-T_c cuprates are determined only by a *single* band, namely, the $dp\sigma$ antibonding band arising from the common CuO_2 plane, which exists in all cases. According to the band calculation,[12] this band has a free-carrier-like wide dispersion and gives rise to a large holelike Fermi surface

enclosing the zone corner. The band calculation, however, often yields additional Fermi surfaces arising from other bands such as Bi-O or Tl-O.[12] If these bands significantly contributed to the transport properties, the transport properties would vary from system to system and hence the universality would be lost. Thus these small electron pockets seem to have little effect on the transport properties. Moreover, since the crystal structure of high-T_c cuprates are not ideal, but include various local defects and distortions, these electron pockets predicted on the basis of ideal structures might not actually exist. In any case, the universal behavior of the transport properties observed in experiments strongly suggests the predominant role of the common CuO_2 band. Therefore we believe that the essential features of the transport properties are well described by the model-band calculation of the CuO_2 plane.

Allen, Pickett, and Krakauer[19] previously calculated the transport properties of $La_{2-x}Sr_xCuO_4$ and $YBa_2Cu_3O_7$ based on local-density-functional theory. They predicted "holelike" R_H (>0) and "electronlike" S (<0) for underdoped and optimally doped regions, which is inconsistent with the experiments, but reminiscent of the behavior in the overdoped region. Although they devoted little discussion to the origin of this apparently unusual behavior, their results clearly demonstrate that the band picture may naturally result in opposite-sign R_H and S for high-T_c cuprates. The disagreement between their results and experiments might be due to the omission of the La^{3+}/Sr^{2+} random potential (virtual-crystal approximation) or to the effect of the CuO chain band. As mentioned above, since the electron correlation makes the band dispersion results less reliable, the full calculation including minor bands may include additional errors. Furthermore, a series problem in the transport calculation including all bands obtained from the band calculation is that it is difficult to get an insight into the phenomenon.

Therefore, in this study, we analyze the tight-binding band model[20,21] for the CuO_2 plane, which is known to reproduce the Fermi-surface morphology consistent with both the band calculations and the photoemission experiments. A striking feature of the CuO_2 antibonding band is that a holelike Fermi surface is formed even when the band is less than half-filled. Thus R_H is always positive. However, as a result of the small band filling, the *band dispersion becomes electronlike.* In other words, the electron on the Fermi surface has an unusual effective mass state in which the "Hall (cyclotron) mass" parallel to the Fermi surface is holelike, but the "transport mass" perpendicular to it is electronlike. This electronlike transport mass contributes to the negative thermopower.

TIGHT-BINDING MODEL AND CALCULATION

In early stages of the study of high-T_c cuprates, Yu, Massidda, and Freeman[20] pointed out that the CuO_2 antibonding band calculated by the full-potential linearized augmented-plane-wave (FLAPW) method is well reproduced by a simple tight-binding band in a two-dimensional (2D) square lattice expressed by

$$E(\mathbf{k}) = -2t_1(\cos k_x a + \cos k_y a) + 4t_2 \cos k_x a \cos k_y a$$

or

$$\varepsilon \equiv E/2t_1 = -(\cos k_x a + \cos k_y a) + 2t \cos k_x a \cos k_y a \ , \tag{1}$$

where t_1 and t_2 are the nearest-neighbor and next-nearest-neighbor interactions, $t = t_2/t_1$, and a is the lattice parameter. Not only t_1, but also t_2 are necessary to describe the CuO_2 band. Although only the Cu-site orbital is considered in Eq. (1), the next-nearest-neighbor interaction t_2 should arise mostly from the O-O direct interaction in the actual CuO_2 plane.

In this study, we use a more realistic tight-binding model in the CuO_2 square lattice consisting of both the Cu $d(x^2-y^2)$ orbital and the O $p\sigma$ orbital, as shown in Fig. 1. The near-neighbor Cu-O and O-O interactions t_{dp} and t_{pp} are taken into account. This model band has been analyzed by Markiewicz.[21] The band structure depends on the relative values of t_{dp}, t_{pp}, and $\Delta E \equiv E_{Cu} - E_O$, the energy difference between d and p oribtals. For $\Delta E \gg t_{dp}$ and t_{pp}, the antibonding band has the same form as Eq. (1), with $t_1 = t_{dp}^2/\Delta E$ and $t_2 = t_1 2t_{pp}/\Delta E$. In the opposite limit $\Delta E = 0$, the constant-energy surface of the antibonding band is given by[21]

$$\cos k_x a = 1 - \frac{\varepsilon(2\varepsilon^2 - 1 + \cos k_y a)}{\varepsilon + \beta(1 - \cos k_y a)} \ , \tag{2}$$

where $\varepsilon = E/2t_{dp}$, $\beta = f(1+\varepsilon f/2)$, and $f = 2t_{pp}/t_{dp}$.

Hereafter, we call the energy bands expressed by Eqs. (1) and (2) as bands A and B, respectively. The more realistic solution of the present tight-binding model shown in Fig. 1 appears to lie between these two limits, because the "bare" values of t_{dp}, t_{pp}, and ΔE are estimated to be 1–1.3, 0.5–0.65, and 1.5–3.6 eV,[22] respectively; hence, $\Delta E \sim t_{dp}, t_{pp}$. Both bands are shown in Fig. 2 together with the Fermi surfaces for various t and f values and band filling n. Both bands show the Van Hove singularity, at $\varepsilon = -2t$ for band A and $\varepsilon = 1$ for B. When n is at the Van Hove singularity, the Fermi surfaces of both bands are exactly the same if

$$2t/(1-2t) = f(1+f/2) \tag{3}$$

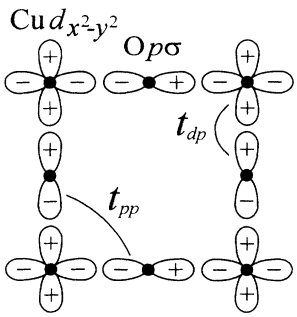

FIG. 1. Tight-binding band model of the CuO_2 plane.

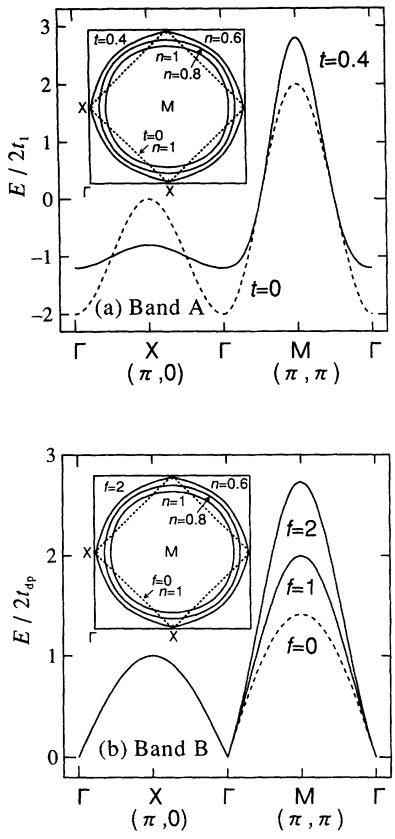

FIG. 2. (a) Band dispersions of band A for $t=0$ and 0.4. The inset shows the Fermi surfaces for $t=0$ at $n=1$ (dotted line) and for $t=0.4$ at $n=1$, 0.8, and 0.6 (solid lines). (b) Band dispersions of band B for $f=0$, 1, and 2. The inset shows the Fermi surfaces for $f=0$ at $n=1$ (dotted line) and for $f=2$ at $n=1$, 0.8, and 0.6 (solid lines).

is satisfied. Even for other n values, it is noted that the Fermi surfaces of both bands are almost identical if Eq. (3) is satisfied, as shown in Fig. 2. At half-filling ($n=1$), the Fermi surface is straight lines if the O-O interaction is ignored ($t=0$ or $f=0$). However, by turning on the O-O interaction, it becomes a holelike rounded shape centered at the Brillouin-zone corner (M), which is similar to that of the band calculation. Such a holelike Fermi surface is formed even at $n=0.6$ for $t=0.4$ or $f=2$. Indeed, a striking feature of the CuO_2 antibonding band is that a holelike Fermi surface is formed even when the band filling is much less than half. According to Yu, Massidda, and Freeman,[20] the Fermi surface from the band calculation is well reproduced with $t=0.45$ for band A, which corresponds to $f=3.36$ for band B. For these values, the holelike Fermi surface is formed even at the smaller n value of 0.5

The Fermi-surface morphology for a given band filling n is solely determined by $t=2t_{pp}/\Delta E$ for band A or $f=2t_{pp}/t_{dp}$ for band B. As mentioned above, the Fermi surfaces for both bands are almost identical if Eq. (3) is satisfied. Therefore we can probably obtain an almost identical Fermi surface as well for the realistic condition $\Delta E \sim t_{dp}, t_{pp}$, by tuning a similar parameter including the O-O direct interaction term t_{pp}. Thus the present tight-binding model shown in Fig. 1 can well reproduce the Fermi-surface morphology predicted from the band calculations and detected in the photoemission experiments.

On the contrary, it is noted that the band dispersions for the two bands are rather different. This difference mainly affects the thermopower S as described below. Although the detailed band structure has not yet been determined by experiments, the actual band dispersion probably lies between those for the two bands. The bandwidth is $8t_1=8t_{dp}^2/\Delta E$ for band A, while it increases with both $2t_{dp}$ and $f=2t_{pp}/t_{dp}$ for band B. Using the above values, one can obtain a bandwidth of ~ 4 eV, which is consistent with the band calculation. However, as mentioned above, the actual bandwidth may be as small as 2 eV. In the present model, one can fit the bandwidth by adjusting t_1 or t_{dp}. In any case, it is noted that the bandwidth does not change the qualitative results of either S or R_H.

R_H and S are calculated based on the conventional Boltzmann transport equations. The energy derivative of the Fermi-Dirac function ($-\partial f/\partial E$) is approximated by a δ function. Thus, considering the square symmetry, T-independent $R_H=\sigma_{xyz}/(\sigma_{xx}\sigma_{yy})$ and T-linear $S=S_{xx}=S_{yy}$ are obtained using

$$\sigma_{xx}=\sigma_{yy}=(e^2/\Omega\hbar)\int \tau(\mathbf{k})v(\mathbf{k})dA \ , \tag{4}$$

$$\sigma_{xyz}=(e^3/\Omega\hbar^2)\int [\tau(\mathbf{k})^2 v(\mathbf{k})^2/r(\mathbf{k})]dA \ , \tag{5}$$

$$S_{xx}(T)=S_{yy}(T)=\frac{\pi^2 k_B^2 T}{3e}\frac{\partial \ln\sigma_{xx}(E)}{\partial E} \ . \tag{6}$$

Here Ω is the normalization volume, $v(\mathbf{k})$ is the electron group velocity, $1/r(\mathbf{k})$ is the curvature of the Fermi surface, and integrals are carried out on the Fermi-surface area. In the calculation, the relaxation time $\tau(\mathbf{k},E)$ is assumed to be constant. This assumption seems to be reasonable for the R_H calculation because the Fermi surface has a symmetrical, rounded shape. In this case, τ is canceled out in both R_H and S. Then R_H is expressed as

$$R_H=(\Omega/e)\left\{\int [v(\mathbf{k})^2/r(\mathbf{k})]dA\right\}\Big/\left\{\int v(\mathbf{k})dA\right\}^2 . \tag{7}$$

Figure 3 shows the band-filling dependence of the calculated $1/n_H \equiv eR_H/a^2$ and S at 300 K for both bands, where n_H is the Hall number per unit cell. In the S calculations, the bandwidth for each band is assumed to be 2 eV. The S value is inversely proportional to this value. In Fig. 3, the parameters $(t,f)=(0,0)$, (0.3,1), and (0.4,2) satisfy Eq. (3), and their Van Hove singularities occur at $n=1$, 0.73, and 0.58, respectively. S diverges at the Van Hove singularity. The behavior of $1/n_H$ for both bands is very similar. This is because R_H is mainly determined by the Fermi-surface curvature, which is nearly identical in both bands. As n decreases from 2, the simple hole picture $n_H=2-n$ holds until near the Van Hove singularity where the Fermi surface touches the Brillouin-zone boundary. Then the shape of the Fermi surface changes

to an electronlike one enclosing the zone center (Γ), followed by the rapid decrease and sign change of R_H.

On the other hand, the band-filling dependences of S for the two bands are considerably different, reflecting the difference in the band dispersions. Equations (4) and (6) show that the sign of S is determined by the sign of $[A(\partial\bar{v}/\partial E)+\bar{v}(\partial A/\partial E)]$ with a constant τ approximation, where $\bar{v}$ is averaged $v(\mathbf{k})$.
Since

$$\frac{\partial v}{\partial E}=\frac{\partial v}{\partial k}\frac{\partial k}{\partial E}=\frac{1}{v\hbar^2}\frac{\partial^2 E}{\partial k^2}=\frac{1}{m^* v},$$

the sign of the first term is determined by the sign of the effective mass $m^*\equiv\hbar^2/(\partial^2 E/\partial k^2)$. As n increases from the band bottom, $m^*>0$ gradually increases and diverges at some inflection point, where m^* changes sign, becoming negative (holelike), and approaches the values at the band top. This sign change of m^* occurs at half-filling (Γ-m direction) for band A with $t=0$, which is consistent with a simple band picture. However, it occurs at a much larger n value of ~ 1.6 for $t=0.4$. For band B whose fermi surface is similar to band A, this sign change occurs at a rather smaller n value. The details will be discussed in the next section. The sign of the second term appears to change near the Van Hove singularity where the Fermi-surface area A is close to the maximum. Therefore the sign change of S could occur between the Van Hove singularity and the mass singularity where m^* diverges. This is clearly demonstrated in Fig. 3(b), where the sign change of S for band A occurs at larger n values than for band B.

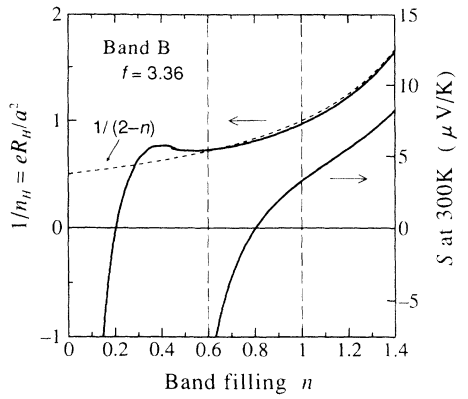

FIG. 4. Band-filling dependences of the inverse Hall number $1/n_H$ and the thermopower S at 300 K for band B with $f=3.36$. The bandwidth is assumed to be 2 eV ($t_{dp}=0.258$ eV). The dashed line indicates the simple hole picture $1/n_H=1/(2-n)$.

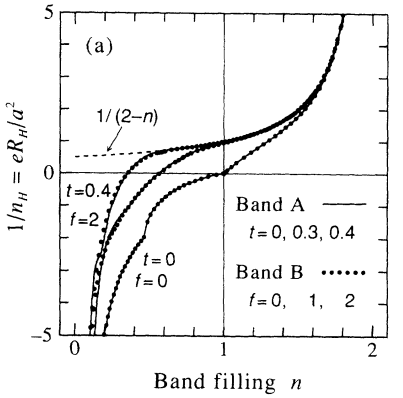

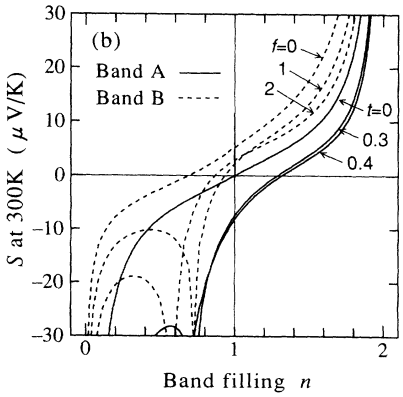

FIG. 3. (a) Band-filling dependences of the inverse Hall number $1/n_H$ for band A with $t=0$, 0.3, and 0.4 (solid lines) and for band B with $f=0$, 1, and 2 (dots). The dashed line indicates the simple hole picture $1/n_H=1/(2-n)$. (b) Band-filling dependences of the thermopower S at 300 K for band A with $t=0$, 0.3, and 0.4 (solid lines) and for band B with $f=0$, 1, and 2 (dashed lines). The bandwidth is assumed to be 2 eV [$t_1=0.25$ eV for band A; $t_{dp}=0.707$ eV ($f=0$), 0.5 eV ($f=1$), and 0.376 eV ($f=2$) or band B].

Qualitatively similar results are obtained even if another approximation of a constant mean free pass $l=\tau v$ is used in the S calculation. In this case, since S is determined by $\partial A/\partial E$, the sign change of S occurs at n near the Van Hove singularity. Then, however, R_H still remains positive for reasonable t or f values, as shown in Fig. 3(a). Thus the sign change of S upon doping occurs earlier than that of R_H.

Figure 4 shows a typical calculated result for band B with $f=3.36$, which reproduces the transport experiments as well as the Fermi-surface morphology obtained from the band calculation. R_H is positive at $n>0.20$, whereas S changes sign at $n\sim 0.80$, which coincides with the optimum hole doping of ~ 0.20.

DISCUSSION

As noted above, the R_H value is almost entirely determined by the Fermi-surface morphology. In particular, the sign of R_H depends on the sign of the Fermi-surface curvature $1/r(\mathbf{k})$ as indicated by Eq. (7). On the other hand, the sign of S is largely affected by the sign of the effective mass m^*, i.e., the curvature of the band dispersion. In the parabolic-band model, both signs should be the same: An electronlike band has a positive m^* as well as a positive Fermi-surface curvature, while a holelike

band has negative ones. On the contrary, the observation of positive R_H and negative S in the overdoped regime implies the existence of an unusual region in which m^* is electronlike (>0) but the Fermi-surface curvature is holelike (<0). This can be understood more clearly in terms of the anisotropic effective-mass tensor. The inverse effective-mass tensor $(1/m^*)_{ij} \equiv \hbar^{-2}(\partial^2 E/\partial k_i \partial k_j)$ on the 2D Fermi surface can be diagonalized with the principal axis perpendicular to the Fermi surface. The above-mentioned effective mass m^* is thus defined as the "transport mass" perpendicular to the Fermi surface, $(1/m^*)_{\rm tr} \equiv \hbar^{-2}(\partial^2 E/\partial k_\perp^2)$, which determines the electron motion along the velocity direction. Another component of the tensor is the "Hall (cyclotron) mass" parallel to the Fermi surface, $(1/m^*)_H \equiv \hbar^{-2}(\partial^2 E/\partial k_\parallel^2)$, which governs the electron motion perpendicular to the velocity (cyclotron motion). Here $k_\perp$ and $k_\parallel$ are the **k**-space coordinates perpendicular and parallel to the Fermi surface, respectively. It is noted that the sign of the Fermi-surface curvature corresponds to the sign of the Hall mass m_H^*.

Therefore the observed anomaly with $R_H > 0$ and $S < 0$ is accompanied by an exceptional electron state in which the Hall mass parallel to the Fermi surface is negative but the transport mass perpendicular to the Fermi surface is positive. This is clearly demonstrated in Fig. 5, where the regions with $m_H^* < 0$ and $m_{\rm tr}^* > 0$ are "painted" with large dots. The half-filled Fermi surfaces are also shown in the figure. When $t = 0$ or $f = 0$, such a mass anomaly appears only in the vicinity of the Van Hove singularity at X. The areas of smaller dots in the figure indicate the reverse anomaly, with $m_H^* > 0$ and $m_{\rm tr}^* < 0$. The symmetrical pattern of Fig. 5(a) is a result of the complete particle-hole symmetry of this band. As t or f is increased, the thickly dotted area rapidly spreads. For band A, the mass anomaly appears in a wide area including the entire half-filled Fermi surface, as shown in Figs. 5(b) and 5(c). For band B, the area develops rather more slowly, but covers the entire half-filled Fermi surface at $f \geq 2$, as shown in Fig. 5(f). It is especially noteworthy that the Fermi surface with the band filling n ranging 0.6–1, which corresponds to that of the high-T_c cuprates in the present model, is completely included in the mass-anomaly area for both bands with realistic parameters ($t \geq 0.4$ or $f \geq 2$). Apparently, this unusual effective-mass state is due to the O-O direct interaction d_{pp} in the CuO_2 plane, which deforms the Fermi surface to a hole-like one even at less than half-filled. Generally speaking, the discrepancy in sign of $m_{\rm tr}^*$ and m_H^* may occur somewhere in the Brillouin zone near half-filling where an electron picture changes to a hole picture. However, it is a rare case that such a mass anomaly occurs *everywhere* on the Fermi surface as demonstrated in the present model. It is very difficult to make such a Fermi surface in a 3D system. The two-dimensional nature of the CuO_2 plane should be significant in this regard.

It is interesting that such a mass anomaly endows the electrons on the Fermi surface with a completely two-faced character: They are electronlike along one direction, but holelike along another direction. This dual character of the electrons may give an answer to a serious

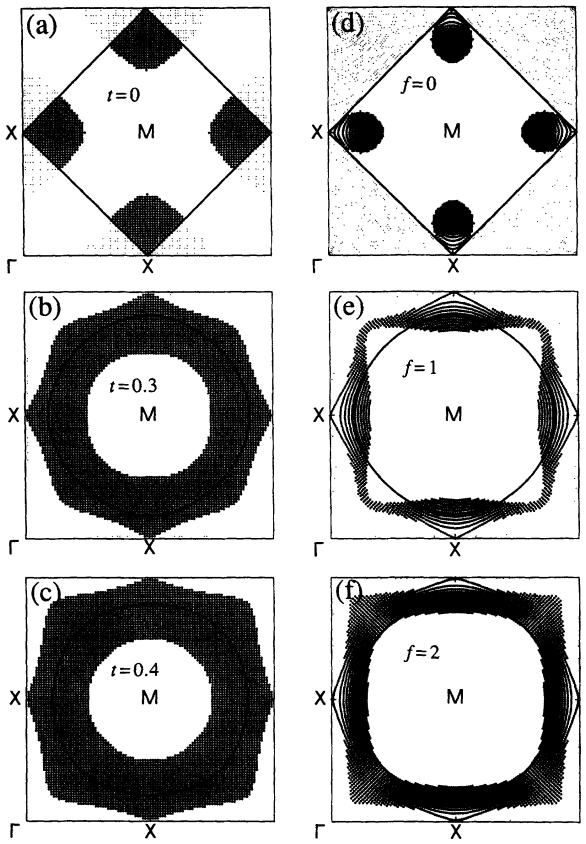

FIG. 5. Mass-anomaly regions with $m_{\rm tr}^* > 0$ and $m_H^* < 0$ are indicated by larger dots, while the reverse regions with $m_{\rm tr}^* < 0$ and $m_H^* > 0$ by smaller dots. (a)–(c) are for band A with $t = 0$, 0.3, and 0.4, and (d)–(f) are for band B with $f = 0$, 1, and 2, respectively. The half-filled Fermi surfaces are also shown by solid lines.

question concerning the nature of the so-called "overdoping." Recently, Niedermayer *et al.*[23] and Uemura *et al.*[24] have measured the muon-spin-rotation (μSR) relaxation rate σ for overdoped $Tl_2Ba_2CuO_{6+\delta}$ (Tl-2201) and found that $\sigma(T \to 0)$ decreases with doping δ. This means, in the framework of the clean-limit London model $\sigma(0) \sim \lambda^{-2} \sim n_s/m^*$, where λ is the magnetic penetration depth and n_s is the superconducting carrier concentration, that n_s/m^* decreases with carrier doping in the overdoped regime. This apparently contradictory result raised a question about the real role of the "overdoping." Now we consider the "carrier concentration" in our model, in which the electrons are two faced. At first, the Hall measurement is mainly governed by the Hall mass, which is holelike. Thus the carrier concentration defined as $n_H \equiv a^2/eR_H$ represents the holelike aspect of the carrier. The "hole doping" expands the holelike Fermi surface area; hence, it increases n_H as if a simple hole picture holds, as shown in Fig. 3(a). On the other hand, the carrier concentration defined from Drude's formula $\sigma = (n/m^*)_D e^2 \tau$ shows a much different behavior, because the conductivity σ is governed by the transport mass and represents the electronlike aspect of the carrier.

From Eq. (4), $(n/m^*)_D \propto \int v(\mathbf{k})dA$ with the constant τ approximation. The electronlike $m^*_{\rm tr}(>0)$ means that the electron velocity $v(\mathbf{k})=\hbar^{-1}\partial E/\partial k$ decreases as the band filling decreases (hole doping). Thus $(n/m^*)_D$ tends to decrease with hole doping while it also depends on the Fermi-surface area. Here it is noted that the sign change of S occurs at the band filling where $(n/m^*)_D \propto \sigma$ becomes maximum, because the energy dependence of σ means the band-filling dependence of σ in our model. Indeed, the sign change of S is the manifestation of the changeover between the hole picture and the electron picture defined from $(n/m^*)_D$. As the band filling increases, $(n/m^*)_D$ increases when $S<0$ (electronlike), but decreases when $S>0$ (holelike). Thus the carrier concentration defined as $(n/m^*)_D$ should decrease with hole doping in the overdoped regime where $S<0$. The superconducting carrier concentration n_s/m^* is defined from the missing area of the optical conductivity $\sigma_1(\omega)$, the spectral weights below the gap frequency transferred to $\omega=0$ as a δ function in the superconducting state. In the clean limit, this missing area is approximately equal to the whole area of $\sigma_1(\omega)$; thus, $n_s/m^* \sim (n/m^*)_D$ using Drude's sum rule. Therefore the superconducting carrier concentration $n_s/m^* \sim (n/m^*)_D$ should decrease with hole doping in the overdoped regime.

In the above scenario, it is noted that $(n/m^*)_D$ becomes maximum at around an optimum doping where $S \sim 0$. However, the experiments show that the dc conductivity $\sigma=(n/m^*)_D e^2\tau$ does not saturate at optimum doping, but continues to increase with doping, even in the overdoped regime. This increase of σ might be attributed to an increase of τ with doping, because some kinds of scattering mechanism, such as spin fluctuations, may be suppressed by the carrier doping. This doping dependence of τ does not contradict the constant-τ approximation in the S calculation, because the latter is assumed for energy dependence at a fixed doping level. In any case, a greater problem in the above scenario is the fact that the μSR results show a rather rapid decrease of n_s/m^* with overdoing, roughly scaling T_c. Further explanation is necessary to attain complete understanding of this rapid decrease of $n_s/m^* \sim (n/m^*)_D$ in the overdoped regime.

The unusual anisotropy in the effective mass may cause significant anisotropy in the scattering process. In that case, we should adopt Anderson's proposal[25] to distinguish two different relaxation times, the transport relaxation time $\tau_{\rm tr}$ and the Hall relaxation time τ_H, which represent, respectively, the relaxation time parallel and perpendicular to the electron velocity. Here they are assumed to be independent of $\mathbf{k}$, as in the above discussion. In this case, $\tau(\mathbf{k})$ in Eq. (4) is written as $\tau_{\rm tr}$, while $\tau(\mathbf{k})^2$ in Eq. (5) as $\tau_{\rm tr}\tau_H$. Thus the R_H expression of Eq. (7) is multiplied by a factor of $(\tau_H/\tau_{\rm tr})$. The inverse Hall mobility is then expressed as

$$\mu_H^{-1} \equiv (\sigma_{xx}R_H)^{-1} = \frac{\tau_H^{-1}(\hbar/e)\int v(\mathbf{k})dA}{\int [v(\mathbf{k})^2/r(\mathbf{k})]dA} . \tag{8}$$

Hence we obtain the relations $\rho \sim \tau_{\rm tr}^{-1}$ and $\mu_H^{-1} \sim \tau_H^{-1}$, just as Anderson did.[25] In this case, the temperature dependence of R_H observed in the experiments can be explained as a simple result of the factor $(\tau_H/\tau_{\rm tr})$, if τ_H and $\tau_{\rm tr}$ have different temperature dependences. Considering the experimental results, this means that τ_H^{-1} is always $\sim T^2$, while $\tau_{\rm tr}^{-1}$ varies from sublinear to superlinear T dependence with carrier doping. In the Anderson model, $\tau_H^{-1} \sim T^2$ can be explained in terms of the spinon-spinon scattering, but $\tau_{\rm tr}^{-1}$ is required to always be T linear due to the holon-spinon scattering. In our Fermi-liquid-like band model, however, the scattering mechanism for both directions should be the same, such as the electron-electron scattering. Thus the temperature dependences of both scattering rates should have the same form, like $\sim T^2$. However, the unusual anisotropy in the effective mass might result in somewhat different scattering mechanisms for both directions, although at present we cannot specify them. Moreover, some possible deviations from the canonical Fermi-liquid model,[26] such as spin fluctuations or weak localization effects, might vary the T dependence of $\tau_{\rm tr}^{-1}$. Further studies on the scattering mechanism will obviously be significant in this regard.

The present tight-binding model does not explain the anomalous T dependence of S observed in the experiments. The $S(T)$ curve generally tends to deviate downwards from the T-linear relation of the simple Fermi liquid. In the underdoped region, $S(T)$ increases linearly with T, but tends to saturate at higher temperature. In the overdoped region, $S(T)$ first increases with T, but immediately decreases at higher temperature, changing its sign to negative. Such $S(T)$ behavior is commonly observed in most high-T_c cuprates. However, in spite of such peculiar T dependence of $S(T)$, the important finding is that the magnitude of S at a given temperature generally decreases with carrier doping.[13–16] This implies that the doping dependence of S is governed by a different mechanism from that for the temperature dependence of S. The present model well explains the general trend in the doping dependence of S. The unusual T dependence of S might be related to some deviations from the canonical Fermi liquid,[26] which do not change the framework of the present band model, but add some special scattering mechanisms to it. In any case, at present it remains impossible to give a consistent explanation for all the T dependences of the transport properties, including ρ, R_H, and S.

In this regard, it seems very important to consider the crystal chemistry of the high-T_c cuprates. Their crystal structure generally consists of two physically different parts: the metallic CuO_2 plane and the ionic charge reservoir (CR) layer. The carriers are at first chemically doped in the CR layer by cation substitution or oxygen nonstoichiometry. Then they are transferred to the CuO_2 plane, becoming itinerant carriers. If the energy level of the carriers in the CR layer is much higher than that in the CuO_2 plane, all doped carriers will be transferred to the CuO_2 plane. However, if the energy levels are close, all carriers might not be transferred to the CuO_2 plane, but some of them might remain in the CR layer as localized carriers. A good example is $YBa_2Cu_3O_7$, where

about half of the hole carriers are believed to remain in the CuO chain layer.[27] The Bi-O or Tl-O layers in the Bi or Tl compounds also have energy levels close to that of the CuO_2 plane.[12] Moreover, the carriers in the ionic CR layer might be trapped by various local defects or even self-trapped as small polarons. Even in $La_{2-x}Sr_xCuO_4$, where the energy level of the La layer is much higher than that of the CuO_2 plane, some of the doped hole carriers might be trapped by the local distortion due to the La^{3+}/Sr^{2+} random potential. Thus the high-T_c cuprates should be considered to be "superlattices" consisting of both metallic (itinerant) and ionic (localized) layers, rather than a physically uniform material. In that case, the trapped carriers in the CR layer might be excited to the CuO_2 plane by a change in, for example, pressure or temperature. Actually, the Hall coefficient of $Tl_2Ba_2CuO_6$ is considerably reduced by about 10%/GPa under pressure,[28] which is attributed to the charge transfer from the Tl-O layer to the CuO_2 plane. Such a large pressure effect of the carrier concentration is never expected for a simple Fermi-liquid-like metal. The CuO_2 plane is not just a simple metal, but a metal existing between the ionic CR layers. Therefore the carrier concentration of the CuO_2 plane could vary with temperature, even if its electronic structure is like a simple Fermi liquid's.[3] Thus the T dependences of the transport properties of the CuO_2 plane would deviate from those of the simple Fermi liquid. The possibility of such T-dependent carrier concentration in high-T_c cuprates has also been discussed by several researchers.[29] If the hole-carrier concentration of the CuO_2 plane is assumed to increase with temperature, as indicated by the R_H data, the unusual $S(T)$ behavior can be qualitatively explained. The present calculation shows that the magnitude of S decreases with hole-carrier doping, from positive to negative, as shown in Fig. 4. Therefore, if the hole-carrier concentration increases with T, the $S(T)$ curve will deviate downwards from simple T-linear behavior at high temperature. In the overdoped regime, $S(T)$ will change sign from positive to negative as T increases.

Finally, it is very interesting to consider the Coulomb interaction between such electrons having the effective-mass anomaly. Since these electrons have complete duality, electronlike in one direction but holelike in another, the Coulomb interaction between them might not necessarily be repulsive. Apparently, this duality of the electron is related to the specific crystal structure of the CuO_2 plane as well as the two dimensionality. However, it is noted that the concept of the effective mass is generally derived from the conventional interaction between the electron and periodic lattice potential. Therefore it may be important to review the nature of the interaction between the electron and periodicity itself.

In conclusion, the doping dependences of both R_H and S of high-T_c cuprates are successfully explained in terms of a tight-binding band model of the CuO_2 square lattice. The essential point is that the band is less than half-filled, but the Fermi surface is still holelike. This brings about an usual electron state in which the Hall mass parallel to the Fermi surface is holelike but the transport mass perpendicular to it is electronlike. This electronlike transport mass contributes to the negative thermopower, while the holelike Hall mass results in a positive Hall coefficient. In such a state, neither a simple hole picture nor a simple electron picture is applicable, although R_H fits the former. The electron on the Fermi surface has a completely two-faced character: It is holelike in one direction, but electronlike in another. In the overdoped regime, where $R_H > 0$ and $S < 0$, hole doping increases the carrier concentration defined as $\propto R_H^{-1}$, but it *decreases* the carrier concentration defined as $(n/m^*)_D$ in Drude's formula. This qualitatively explains the recent μSR results that the superconducting carrier concentration $n_s/m^* \sim (n/m^*)_D$ decreases with hole doping in the overdoped regime. Such an unusual, complicated electron state apparently originates in the peculiar band structure of the CuO_2 plane. Thus the sign change of S upon doping observed in experiments is strong evidence for the validity of the band picture. It is noted that high-T_c superconductivity appears in the region with such an effective-mass anomaly. This unusual effective-mass state formed in the CuO_2 band at around half-filling might play a role in the high-T_c superconductivity mechanism.

ACKNOWLEDGMENTS

The author thanks N. Hamada, T. Manako, T. Kondo, and M. Mizuta for helpful discussions.

[1]For a review, see Y. Iye, in *Physical Properties of High Temperature Superconductors,* edited by D. M. Ginsberg (World Scientific, Singapore, 1992).

[2]T. R. Chien, Z. Z. Wang, and N. P. Ong, Phys. Rev. Lett. **67**, 2088 (1991).

[3]Y. Kubo and T. Manako, Physica C **197**, 378 (1992).

[4]G. Xiao, P. Xiong, and M. Z. Cieplak, Phys. Rev. B **46**, 8687 (1992).

[5]C. Kendziora, D. Mandrus, L. Mihaly, and L. Forro, Phys. Rev. B **46**, 14 297 (1992).

[6]P. S. Wang, J. C. Williams, K. D. D. Rathnayaka, B. D. Hennings, D. G. Naugle, and A. B. Kaiser, Phys. Rev. B **47**, 1119 (1993).

[7]A. Carrington, A. P. Mackenzie, C. T. Lin, and J. R. Cooper, Phys. Rev. Lett. **69**, 2855 (1992).

[8]W. Jiang, J. L. Peng, S. J. Hagen, and R. L. Greene, Phys. Rev. B **46**, 8694 (1992).

[9]J. M. Harris, Y. F. Yan, and N. P. Ong, Phys. Rev. B **46**, 14 293 (1992).

[10]B. Wuyts, E. Osquiguil, M. Maenhoudt, S. Libbrecht, Z. X. Gao, and Y. Bruynseraede, Phys. Rev. B **47**, 5512 (1993).

[11]P. Xiong, G. Xiao, and X. D. Wu, Phys. Rev. B **47**, 5516 (1993).

[12]For a review, see W. E. Pickett, Rev. Mod. Phys. **61**, 433 (1989).

[13]K. Matsuura, T. Wada, Y. Yaegashi, S. Tajima, and H.

Yamauchi, Phys. Rev. B **46**, 11 923 (1992).
[14]S. D. Obertelli, J. R. Cooper, and J. L. Tallon, Phys. Rev. B **46**, 11 928 (1992).
[15]C. K. Subramaniam, A. B. Kaiser, H. J. Trodahl, A. Mawdsley, and R. G. Buckley, Physica C **203**, 98 (1992).
[16]C. R. Varoy, H. J. Trodahl, R. G. Buckley, and A. B. Kaiser, Phys. Rev. B **46**, 463 (1992).
[17]T. Takahashi *et al.*, Nature **334**, 691 (1988); C. G. Olson *et al.*, Science **245**, 731 (1989); J. C. Campuzano *et al.*, Phys. Rev. Lett. **64**, 2308 (1990).
[18]D. M. King *et al.*, Phys. Rev. Lett. **70**, 3159 (1993); R. O. Anderson *et al.*, *ibid.* **70**, 3163 (1993).
[19]P. B. Allen, W. E. Pickett, and H. Krakauer, Phys. Rev. B **37**, 7482 (1988); in *Novel Superconductivity,* edited by S. A. Wolf and V. Z. Kresin (Plenum, New York, 1987), p. 489.
[20]J. Yu, S. Massidda, and A. J. Freeman, Physica C **152**, 273 (1988).
[21]R. S. Markiewicz, J. Phys. Condens. Matter **1**, 8911 (1989).
[22]E. B. Stechel and D. R. Jennison, Phys. Rev. B **38**, 8873 (1988); M. S. Hybertsen and M. Schlüter, *ibid.* **39**, 9028 (1989).
[23]Ch. Niedermayer, C. Brenhard, U. Binninger, H. Glückler, J. L. Tallon, E. J. Ansaldo, and J. I. Budnick, Phys. Rev. Lett. **71**, 1764 (1993).
[24]Y. J. Uemura, A. Keren, L. P. Le, G. M. Luke, W. D. Wu, Y. Kubo, T. Manako, Y. Shimakawa, M. Subramanian, J. L. Cobb, and J. T. Markert, Nature **364**, 605 (1993).
[25]P. W. Anderson, Phys. Rev. Lett. **67**, 2092 (1991).
[26]For a review, see K. Levin, J. H. Kim, J. P. Lu, and Q. Si, Physica C **175**, 449 (1991).
[27]Y. Tokura *et al.*, Phys. Rev. B **38**, 7156 (1988).
[28]H. Takahashi, A.-K. Klehe, C. Looney, J. S. Schilling, N. Môri, Y. Shimakawa, Y. Kubo, and T. Manako, Physica C **217**, 163 (1993).
[29]V. V. Moshchalkov, Solid State Commun. **73**, 777 (1990); J. E. Hirsch *et al.*, Physica C **195**, 355 (1992).

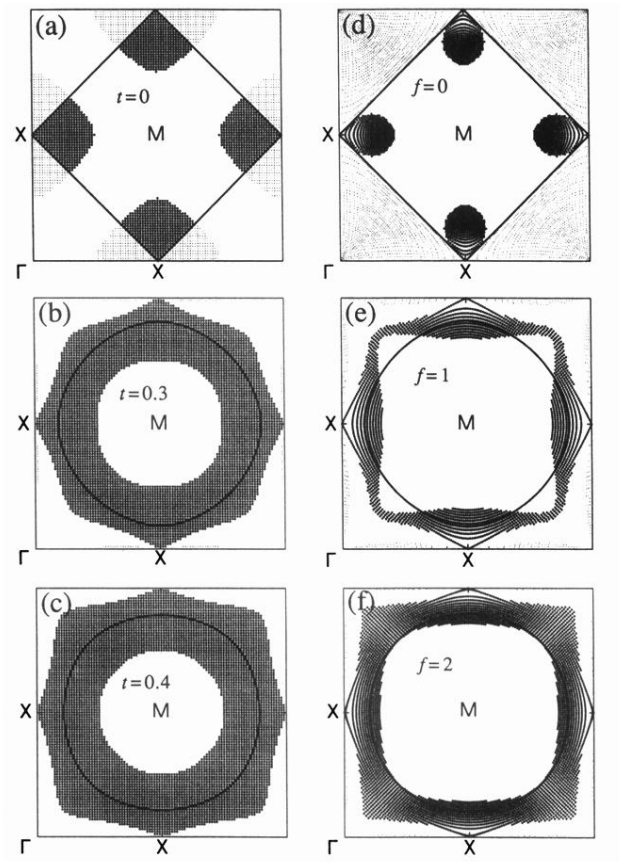

FIG. 5. Mass-anomaly regions with $m^*_{\rm tr}>0$ and $m^*_H<0$ are indicated by larger dots, while the reverse regions with $m^*_{\rm tr}<0$ and $m^*_H>0$ by smaller dots. (a)–(c) are for band A with $t=0$, 0.3, and 0.4, and (d)–(f) are for band B with $f=0$, 1, and 2, respectively. The half-filled Fermi surfaces are also shown by solid lines.